FEBS Letters 583 (2009) 739–742

FEBS Letters

journal homepage: www.FEBSLetters.org

Probing the orientation of yeast VDAC1 in vivo

Beth M. McDonald [a,b], Mateusz M. Wydro [b], Robert N. Lightowlers [b], Jeremy H. Lakey [a,*]

[a] The Institute for Cell and Molecular Biosciences, Newcastle University, Framlington Place, Newcastle-upon-Tyne NE2 4HH, UK
[b] Mitochondrial Research Group, Newcastle University, Framlington Place, Newcastle-upon-Tyne NE2 4HH, UK

ARTICLE INFO

Article history:
Received 11 December 2008
Revised 13 January 2009
Accepted 14 January 2009
Available online 29 January 2009

Edited by Peter Brzezinski

Keywords:
Voltage dependent anion channel
Mitochondrial porin
Structure
Immunoprecipitation
Yeast

ABSTRACT

Voltage dependent anion channel (VDAC) is a vital ion channel in mitochondrial outer membranes and its structure was recently shown to be a 19 stranded β-barrel. However the orientation of VDAC in the membrane remains unclear. We probe here the topology and membrane orientation of yeast *Saccharomyces cerevisiae* in vivo. Five FLAG-epitopes were independently inserted into scVDAC1 and their surface exposure in intact and disrupted mitochondria detected by immunoprecipitation. Functionality was confirmed by measurements of respiration. Two epitopes suggest that VDAC (scVDAC) has its C-terminus exposed to the cytoplasm whilst two others are more equivocal and, when combined with published data, suggest a dynamic behavior.

1. Introduction

Voltage dependent anion channel (VDAC), forms large channels across the outer mitochondrial membrane (OMM) and occurs in up to three isoforms per eukaryotic species [1]. VDAC is essential for the exchange of mitochondrial cofactors and essential metabolites (such as succinate, citrate, phosphate, NADH and ATP) [2,3]. The channel is open and anion selective at low transmembrane potentials, enabling permeation of molecules <6–8 kDa [4]. However, at high potentials, it changes to a cation selective 'closed state', preventing permeability of anions such as ATP. It has also been suggested to play a role in apoptosis [5] although this remains controversial [6]. Despite its importance, the structure of VDAC1 was unclear [7–10] until recently published high resolution structures of human and mouse VDAC1 revealed a 19 stranded β-barrel capable of dimerization and dynamic fluctuation [11–13] (Fig. 1). However, the orientation of VDAC in the mitochondrial membrane is unclear.

Sequence alignments show a 58% similarity between yeast and hVDAC1 and 71% between yeast and *nc*VDAC1. Furthermore, residues thought to be important for the structure and function of VDAC occupy similar positions [8,14]. Therefore, this work is based upon the hypothesis that VDAC1 adopts a similar structure in yeast and human mitochondria. Antibody binding to FLAG-epitopes (DYKDDDDK) indicates their surface exposure [15,16] and FLAG was placed in selected regions of VDAC and probed by immunoprecipitation (IP) [11–13,17].

2. Materials and methods

2.1. Cloning and site-directed mutagenesis for FLAG-epitope insertion

The *Saccharomyces cerevisiae* VDAC1 (scVDAC1) gene and its promoter sequence (YNL055C coordinates 518997–517742, chromosome XIV), was amplified by PCR from genomic DNA, purified and blunt-end ligated into yeast shuttle vector YCPlac22 previously digested with *Sma*I (Promega) and treated with alkaline phosphatase. Quikchange mutagenesis (Stratagene, UK) was used to create five independent scVDAC1-FLAG variants according to manufacturer's instructions. *Escherichia coli* transformants were screened for the correct mutation by colony PCR. Sequences were confirmed in all cases by automated sequence analysis (Lark technologies, UK).

2.2. Oxygraph high resolution cell respirometry

Respiratory analysis was carried out using the Oxygraph 2000 system (Oroboros, Austria). M22-2 (Δ*por1*) *S. cerevisiae* containing VDAC1-FLAG-YCPlac22 variants were streaked onto YEPGE plates

Abbreviations: OMM, outer mitochondrial membrane; IMS, intermembrane space; scVDAC, *Saccharomyces cerevisiae* VDAC; hsVDAC, human VDAC; IP, immunoprecipitation

* Corresponding author. Fax: +44 191 222 7424.
E-mail address: J.H.Lakey@newcastle.ac.uk (J.H. Lakey).

0014-5793/$34.00
doi:10.1016/j.febslet.2009.01.039

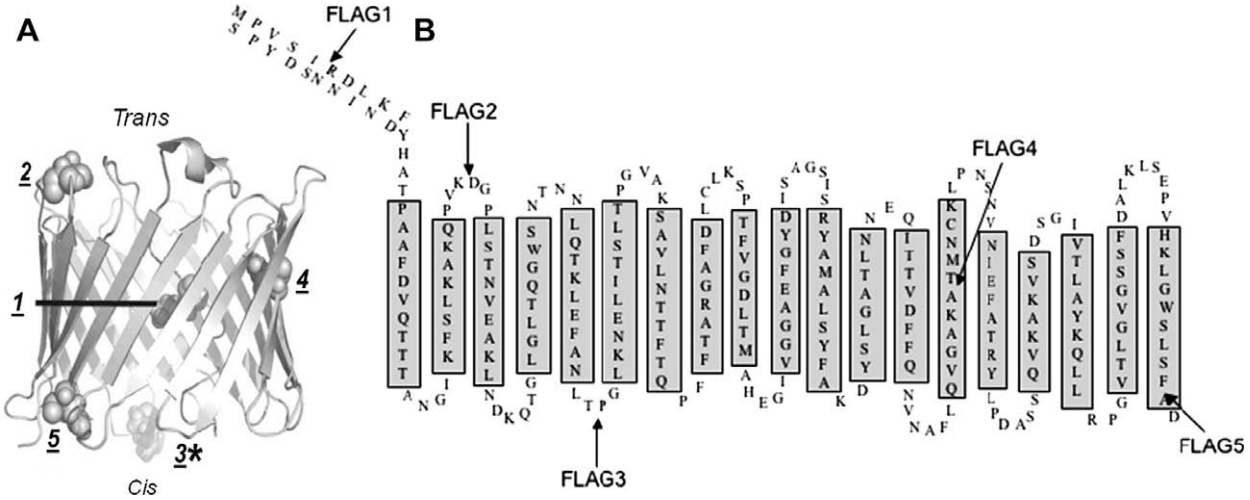

Fig. 1. VDAC1 structure and FLAG-epitope positions. (A) Three-dimensional model of hsVDAC1 drawn with Pymol [DeLano Scientific] using PDB coordinates 2K4T from [11] (see also 2JK4 [12] and 3EMN [13]) indicating FLAG-epitope locations used in the current study (1–5). FLAG3, which contradicts the structure, is highlighted (∗). (B) scVDAC1 model based on the hsVDAC1 structure with FLAG positions indicated. Rectangles represent transmembrane regions.

and were grown at 30 °C for 48 h. Wild-type M3 parental *S. cerevisiae* (positive control) and M22-2 (Δ*por1*) *S. cerevisiae* (negative control) were grown under the same conditions. Cells were resuspended in sterile PBS, 3% glycerol and counted using a CASY Schärfe cell counter (Casy Technology Reutlingen, Germany) with analyser system (Model TT). The oxygen consumption rate (pmol/s/million cells) for each sample was calculated using Oroboros DatLab version 4 software.

2.3. Mitochondrial isolation, immunoprecipitation (IP) and western blotting

M22-2 cells were transformed with YCPlac22-scVDAC-FLAG variants 1–5, respectively, following procedures described in [18]. Variants were plated onto minimal agar (-Trp to select for the YCPlac22 plasmid and -Leu to maintain Δ*por1*) and were incubated for 48 h at 30 °C. 2 × 500 ml cultures of yeast hosting each of the recombinant-FLAG plasmids were grown to an $OD_{600} \approx 0.2$ and cells were harvested by centrifugation at 2500×*g* for 5 min at room temperature. Whole mitochondria were isolated from *S. cerevisiae* as described in [19] and protein concentration of mitochondrial fractions determined by Bradford assay.

Anti-FLAG M2 monoclonal antibody (A2220, Sigma) bound to agarose beads was centrifuged at 5000×*g* for 30 s to remove storage buffer. For each sample, 40 μl beads were washed and equilibrated three times with 1 ml SH buffer (0.6 M Sorbitol, 20 mM HEPES–KOH pH 7.4) centrifuging as before. Fresh mitochondria (200 μg per FLAG-VDAC variant) were resuspended in ice cold SH buffer to a final volume of 500 μl. For "disrupted mitochondria", an identical sample was solubilised in 1% v:v Triton X-100/SH buffer (final volume 500 μl) until the solution clarified. 'Intact' and 'disrupted' fractions were mixed separately with anti-FLAG beads, incubated for 4 h on a rotating drum at 4 °C, pelleted by centrifugation at 5000×*g* for 30 s at 2 °C, and unbound material discarded in the supernatant. Beads were similarly washed twice with 1 ml cold SH buffer and then with ice cold PBS 1% v:v Triton X-100 for 5 min at 4 °C on a rotating drum to solubilise bound mitochondria to leave just FLAG-tagged VDAC attached to the beads. All beads were washed a final time with 1 ml PBS 1% v:v Triton X-100 by inverting the tubes several times and samples pelleted as before.

After separation on SDS–PAGE, proteins were transferred onto a PVDF membrane by wet transfer, blocked in 5% milk/TTBS (20 mM Tris, 0.5 M NaCl, 0.1% Tween-20) overnight at 4 °C, washed three times in TTBS and probed with anti-VDAC polyclonal (*Neurospora crassa*) antisera. Membranes were washed three times then incubated with HRP-conjugated porcine anti-rabbit IgG (P0399, Dako Cytomation). After a final three washes, the blots were developed using ECL+ reagents for 5 min and imaged on a Storm Phosphoimager (GE Healthcare).

3. Results and discussion

3.1. Localization of FLAG-tagged VDAC1

Translocation and assembly of scVDAC1-FLAG variants (Fig. 1) into the mitochondria of M22-2 Δ*por1* (VDAC1-deficent) cells was confirmed by western blot (Fig. 2). Isolated mitochondrial and cytosolic fractions were probed with anti-FLAG, anti-VDAC and anti-PGK antibodies with wild-type VDAC1 from M3 (parental) strain as a control. All scVDAC1-FLAG variants were identified in mitochondrial fractions and not in the cytosol (Fig. 2, row 2). Prob-

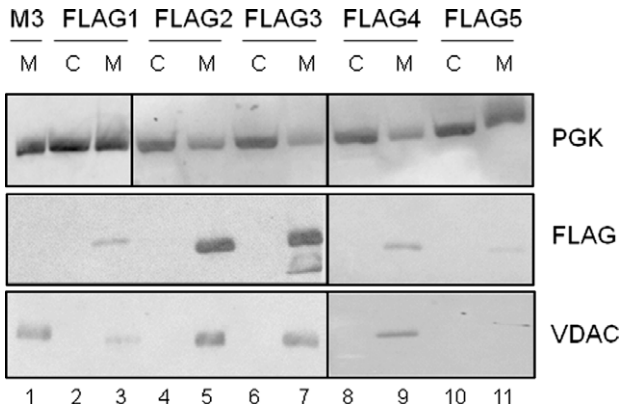

Fig. 2. FLAG-tagged VDAC1 variants are localized to mitochondria. Mitochondrial (M) and cytosolic (C) fractions were prepared from M3 parental control strain and all five variants of VDAC1 (FLAG1-5) as described in materials and methods. Aliquots (2 μg) were subjected to western blot analysis with antibodies raised against VDAC1 or the FLAG peptide, as indicated. Enrichment for mitochondrial fractions was confirmed by probing for the cytosolic marker enzyme posphoglycerate kinase (PGK), some of which remains attached to the mitochondria (PGK, lanes 1, 3, 5, 7, 9 and 11).

ing with anti-PGK (cytosolic) confirmed effective mitochondrial – cytosolic separation.

3.2. Functional studies of FLAG-inserted VDAC variants in vivo

To determine whether the insertion of a charged FLAG-epitope affected the native structure of VDAC1, respiration of M3 wild-type and M22-2 Δ*por1* cells alone or hosting VDAC1-FLAG variants, was measured by respirometry in 12 parallel experiments (Fig. 3). M22-2 retained a minimal flux of 22.3 ± 4.1 pmol/s/million cells which was increased by the endogenous expression of VDAC1 in the M3 wild-type control to 30.3 ± 4.4 pmol/s/million cells. When compared to the respiratory rate for the M3 wild-type control, variants 1–5 recovered between 70% and 125% of oxygen flux in M22-2. For each variant, the rescue of respiratory rate was statistically significant and this is our strongest evidence that the FLAG inserts do not induce large structural changes. Differences in the amounts of VDAC1-FLAG consistently found between strains (Fig. 3, M3 *cf.* FLAG1) did not correlate with the respiratory rate. The control that VDAC1 exerts on the respiration rate (control strength) is unknown but probably minimal. Consequently, restoration of even low levels of functional VDAC1 may be sufficient to restore normal respiratory rates.

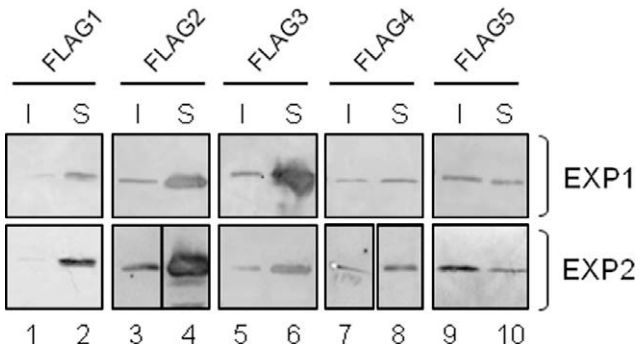

Fig. 4. Immunoprecipitation of solubilised and intact mitochondria hosting VDAC1-FLAG variants in the OMM. Equal amounts of intact (I) or solubilised (S) mitochondria isolated from strains expressing individual VDAC1-FLAG variants were subjected to immunoprecipitation assays with beads decorated with anti-FLAG antibodies as detailed in materials and methods. VDAC1 variants were eluted from the beads and subjected to western blot analysis with anti-VDAC1 antibody. EXP1 and EXP2 refer to separate repeat experiments. For each variant, samples precipitated from the intact and solubilised mitochondria were loaded on the same gel and transferred to the same membrane. However, in EXP2 samples from the solubilised and intact mitochondria of FLAG2 and 4 variants were not loaded in sequential lanes.

3.3. Immunoprecipitation of intact and disrupted mitochondria

The terms *cis* and *trans* sides of VDAC are used here for clarity and defined in Fig. 1. Mitochondria containing VDAC1-FLAG variants were incubated with anti-FLAG antibody bound to agarose beads. VDAC1-FLAG1 did not bind antibody in intact mitochondria (Fig. 4, lane 1 *cf.* 2). This suggests that the intact OMM prevented access to the FLAG1-epitope [15]. In contrast, VDAC1-FLAG5 showed equal levels of binding (Fig. 4, lane 9 *cf.* 10), consistent with a cytosolic location. Binding of FLAG5 in both intact and disrupted mitochondria was low but this reflects its abundance in the OMM (Fig. 2, lane 11) Nevertheless, a 98% recovery in respiration rate confirmed that VDAC1-FLAG5 is functional (Fig. 3).

VDAC-FLAG2 and FLAG3 are on the *trans* and *cis* sides of VDAC1 respectively and both bound antibody before membrane solubilization but much more strongly afterwards. This discrimination is less distinct than with FLAG1 and shows that both the *cis* and *trans* epitopes are partially exposed before solubilization but revealed more clearly after.

By comparison, FLAG4 showed a much smaller increase in binding in solubilised mitochondria in comparison to the intact organelle (Fig. 4, lanes 7 and 8). Levels of binding in both samples were minimal even though FLAG4 is abundant in the OMM (Fig. 2). This lack of exposure is consistent with a FLAG-epitope located in a transmembrane segment that is occluded by membrane in intact mitochondria or micelles in the disrupted state.

The clearest data are thus obtained from FLAG1 and 5. In FLAG1 minimal binding in intact, and strong binding in disrupted, mitochondria indicates an IMS exposure in agreement with published data [20] and its known exposure to the aqueous phase [7,21]. The remaining epitopes reported in the only other study of orientation in intact mitochondria [20] are shown by the recent structures to be mostly buried in membrane strands and therefore difficult to interpret. In the published structures [11–13] the N-terminal segment first exits the membrane on the *trans* side [11,12] before folding through the lumen to almost reach the *cis* side [13]. The FLAG1, which is 11–20 residues from the N-terminus, will most likely have a *trans* exposure (see Fig. 1); especially if the N-terminus is as dynamic as proposed [8,13,22–25]. Residues 1–10 continue through the lumen towards exposure of the extreme N-terminal residue to the cis side. The equal binding of C-terminal FLAG5 to solubilised and intact OMM indicates a cytosolic location for this *cis* side. This places the VDAC in the opposite orientation to that proposed by Bayrhuber et al. [12], which is thought to resemble the bacterial OMP orientation.

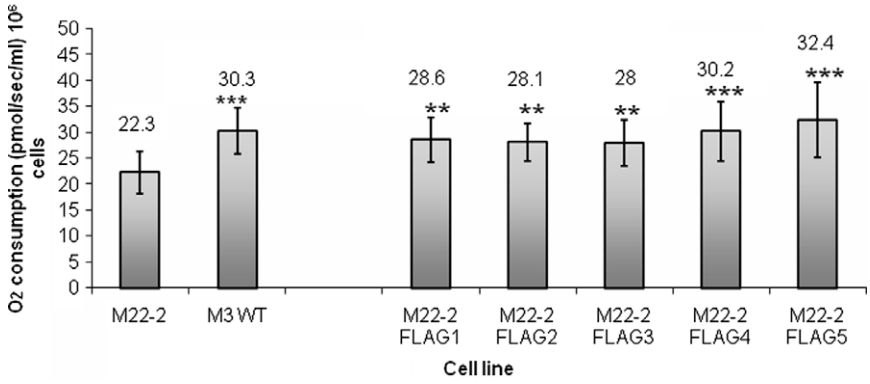

Fig. 3. Respiration rates of WT and M22-2 (Δpor1) S. cerevisiae and M22-2 hosting VDAC1-FLAG variants. Cell lines were grown in non-fermentable carbon sources and analyzed for rates of cellular respiration as described in materials and methods. Rates for all strains were measured on 12 separate occasions from different preparations. Statistical significance was calculated by comparing values against M22-2 Δ*por1* in an unpaired students *t*-test ($^{*}0.05 > P > 0.01$; $^{**}0.01 > P > 0.001$; and $^{***}0.001 > P$).

The unexpected results of FLAG2 and 3 (Fig. 5a *cf.* b), which according to the structure papers should be cytosolic and IMS, respectively, lack ready explanation. It is possible that there is a slight difference in structure between yeast and mammalian VDAC1 as their sequence homology is low. Interestingly, this region in VDAC1 is less well resolved in the first NMR derived structure with fewer NOEs [11] and is located in a dynamic region in the second structure, that has high rates of hydrogen/deuterium exchange [12]. Furthermore, other studies [21,26] have shown residues within this region to be more water exposed than suggested by the published structures (illustrated in Supplementary data). Finally it should be noted that our data concurs with the 13 β-stranded model deduced from functional studies [26].

In conclusion two FLAG-epitopes have defined the orientation of the solved structures in vivo with the C-terminus facing the cytosol. One more confirms its expected transmembrane position. The two remaining epitopes behave similarly in the IP although they should be on opposite sides of the membrane. This curious result does however concur with previous data and together they suggest that β-strands 1–6 are dynamic [27–29] and require further investigation.

Acknowledgments

We thank the BBSRC for Committee Studentship (BBS/S/A/2004/10912), Dr. Roland Lill (Phillips Universtiat, Marburg, Germany) for supplying Anti-VDAC antibody (*N. crassa*), Mike Forte for supplying M22-2 (M3 Δ*por1*), Brian Morgan for sharing knowledge and for supplying YCPlac22, to Jeremy Brown and colleagues for support and Helen Ridley for technical support.

Appendix A. Supplementary data

Supplementary data associated with this article can be found, in the online version, at doi:10.1016/j.febslet.2009.01.039.

References

[1] Colombini, M. (2004) VDAC: the channel at the interface between mitochondria and the cytosol. Mol. Cell. Biochem. 256–257, 107–115.
[2] Hodge, T. and Colombini, M. (1997) Regulation of metabolite flux through voltage-gating of VDAC channels. J. Membr. Biol. 157, 271–279.
[3] Zizi, M., Forte, M., Blachly-Dyson, E. and Colombini, M. (1994) NADH regulates the gating of VDAC, the mitochondrial outer membrane channel. J. Biol. Chem. 269, 1614–1616.
[4] Benz, R. (1994) Permeation of hydrophilic solutes through mitochondrial outer membranes: review on mitochondrial porins. Biochim. Biophys. Acta 1197, 167–196.
[5] Shimizu, S., Ide, T., Yanagida, T. and Tsujimoto, Y. (2000) Electrophysiological study of a novel large pore formed by Bax and the voltage-dependent anion channel that is permeable to cytochrome c. J. Biol. Chem. 275, 12321–12325.
[6] Baines, C.P., Kaiser, R.A., Sheiko, T., Craigen, W.J. and Molkentin, J.D. (2007) Voltage-dependent anion channels are dispensable for mitochondrial-dependent cell death. Nat. Cell Biol. 9, 550–555.
[7] Casadio, R., Jacoboni, I., Messina, A. and De Pinto, V. (2002) A 3D model of the voltage-dependent anion channel (VDAC). FEBS Lett. 520, 1–7.
[8] Blachly-Dyson, E., Peng, S., Colombini, M. and Forte, M. (1990) Selectivity changes in site-directed mutants of the VDAC ion channel: structural implications. Science 247, 1233–1236.
[9] Forte, M., Adelsberger-Mangan, D. and Colombini, M. (1987) Purification and characterization of the voltage-dependent anion channel from the outer mitochondrial membrane of yeast. J. Membr. Biol. 99, 65–72.
[10] Rauch, G. and Moran, O. (1994) On the structure of mitochondrial porins and its homologies with bacterial porins. Biochem. Biophys. Res. Commun. 200, 908–915.
[11] Hiller, S., Garces, R.G., Malia, T.J., Orekhov, V.Y., Colombini, M. and Wagner, G. (2008) Solution structure of the integral human membrane protein VDAC-1 in detergent micelles. Science 321, 1206–1210.
[12] Bayrhuber, M. et al. (2008) Structure of the human voltage-dependent anion channel. Proc. Natl. Acad. Sci. USA 105, 15370–15375.
[13] Ujwal, R., Cascio, D., Colletier, J.P., Faham, S., Zhang, J., Toro, L., Ping, P. and Abramson, J. (2008) The crystal structure of mouse VDAC1 at 2.3 A resolution reveals mechanistic insights into metabolite gating. Proc. Natl. Acad. Sci. USA 105, 17742–17747.
[14] Jeanteur, D., Lakey, J.H. and Pattus, F. (1991) The bacterial porin superfamily: sequence alignment and structure prediction. Mol. Microbiol. 5, 2153–2164.
[15] Visudtiphole, V., Chalton, D.A., Hong, Q. and Lakey, J.H. (2006) Determining OMP topology by computation, surface plasmon resonance and cysteine labelling: the test case of OMPG. Biochem. Biophys. Res. Commun. 351, 113–117.
[16] Mao, Q., Foster, B.J., Xia, H. and Davidson, B.L. (2003) Membrane topology of CLN3, the protein underlying Batten disease. FEBS Lett. 541, 40–46.
[17] McDonald, B. (2008) A study of the folding and topology of VDAC isoforms from *Saccharomyces cerevisiae*. PhD Thesis. Newcastle University.
[18] Ito, H., Fukuda, Y., Murata, K. and Kimura, A. (1983) Transformation of intact yeast cells treated with alkali cations. J. Bacteriol. 153, 163–168.
[19] Diekert, K., de Kroon, A.I., Kispal, G. and Lill, R. (2001) Isolation and subfractionation of mitochondria from the yeast *Saccharomyces cerevisiae*. Meth. Cell Biol. 65, 37–51.
[20] Stanley, S., Dias, J.A., D'Arcangelis, D. and Mannella, C.A. (1995) Peptide-specific antibodies as probes of the topography of the voltage-gated channel in the mitochondrial outer membrane of *Neurospora crassa*. J. Biol. Chem. 270, 16694–16700.
[21] Engelhardt, H., Meins, T., Poynor, M., Adams, V., Nussberger, S., Welte, W. and Zeth, K. (2007) High-level expression, refolding and probing the natural fold of the human voltage-dependent anion channel isoforms I and II. J. Membr. Biol. 216, 93–105.
[22] De Pinto, V. et al. (2007) Determination of the conformation of the human VDAC1 N-terminal peptide, a protein moiety essential for the functional properties of the pore. Chembiochem 8, 744–756.
[23] Colombini, M., Blachly-Dyson, E. and Forte, M. (1996) VDAC, a channel in the outer mitochondrial membrane. Ion Channels 4, 169–202.
[24] Popp, B., Court, D.A., Benz, R., Neupert, W. and Lill, R. (1996) The role of the N and C termini of recombinant Neurospora mitochondrial porin in channel formation and voltage-dependent gating. J. Biol. Chem. 271, 13593–13599.
[25] Guo, X.W., Smith, P.R., Cognon, B., D'Arcangelis, D., Dolginova, E. and Mannella, C.A. (1995) Molecular design of the voltage-dependent, anion-selective channel in the mitochondrial outer membrane. J. Struct. Biol. 114, 41–59.
[26] Song, J., Midson, C., Blachly-Dyson, E., Forte, M. and Colombini, M. (1998) The topology of VDAC as probed by biotin modification. J. Biol. Chem. 273, 24406–24413.
[27] Dolder, M., Zeth, K., Tittmann, P., Gross, H., Welte, W. and Wallimann, T. (1999) Crystallization of the human, mitochondrial voltage-dependent anion-selective channel in the presence of phospholipids. J. Struct. Biol. 127, 64–71.
[28] Guo, X.W. and Mannella, C.A. (1993) Conformational change in the mitochondrial channel, VDAC, detected by electron cryo-microscopy. Biophys. J. 64, 545–549.
[29] Peng, S., Blachly-Dyson, E., Forte, M. and Colombini, M. (1992) Large scale rearrangement of protein domains is associated with voltage gating of the VDAC channel. Biophys. J. 62, 123–131.